Exposing strangeness: Projections for kaon electromagnetic form factors

Fei Gao,[1,2,*] Lei Chang,[3,†] Yu-Xin Liu,[1,2,4,‡] Craig D. Roberts,[5,§] and Peter C. Tandy[6,‖]

[1]*Department of Physics and State Key Laboratory of Nuclear Physics and Technology, Peking University, Beijing 100871, China*
[2]*Collaborative Innovation Center of Quantum Matter, Beijing 100871, China*
[3]*School of Physics, Nankai University, Tianjin 300071, China*
[4]*Center for High Energy Physics, Peking University, Beijing 100871, China*
[5]*Physics Division, Argonne National Laboratory, Argonne, Illinois 60439, USA*
[6]*Center for Nuclear Research, Department of Physics, Kent State University, Kent, Ohio 44242, USA*

(Received 14 March 2017; published 28 August 2017)

A continuum approach to the kaon and pion bound-state problems is used to reveal their electromagnetic structure. For both systems, when used with parton distribution amplitudes appropriate to the scale of the experiment, Standard Model hard-scattering formulas are accurate to within 25% at momentum transfers $Q^2 \approx 8$ GeV^2. There are measurable differences between the distribution of strange and normal matter within the kaons, e.g. the ratio of their separate contributions reaches a peak value of 1.5 at $Q^2 \approx 6$ GeV^2. Its subsequent Q^2 evolution is accurately described by the hard scattering formulas. Projections for the ratio of kaon and pion form factors at timelike momenta beyond the resonance region are also presented. These results and projections should prove useful in planning next-generation experiments.

DOI: 10.1103/PhysRevD.96.034024

I. INTRODUCTION

Kaons and strange quarks are a bridge between strong and electroweak interactions. For instance, they opened the first window on CP violation, responsible for the matter-antimatter asymmetry in our Universe, and characterize strong interactions in a sector where the Higgs-generated quark current mass cannot be treated as a perturbation, i.e. a domain where flavor dependence of the strong interaction becomes important and measurable. Indeed, at perturbative Standard-Model (SM) scales the strange-to-up + down quark mass ratio is $2m_s/[m_u + m_d] = 27.3(7)$ [1]; but, as the resolving scale is reduced, this ratio evolves so that, in the far infrared, its value is much smaller (∼1.2–1.5 [2–4]) owing to emergent phenomena peculiar to the strong interaction. Consequently, comparisons between kaon and pion properties provide direct access to the interplay between strong and electroweak mass-generating mechanisms. Such qualities make the kaon a tantalizing subject for study, providing a challenging target for both experiment and theory, and demanding that connections be drawn between them.

There are four types of kaon: $K^{\pm}$, K^0, $\bar{K}^0$, whose valence-quark content is, respectively, $u\bar{s}$, $\bar{u}s$, $d\bar{s}$, $\bar{d}s$, where $\bar{q}$ identifies an antiquark; and, within the SM's strong-interaction sector, quantum chromodynamics (QCD), one of the most pressing empirical challenges is to map the distribution of electric charge within the kaons. Since the charge of u- and s-quarks is different, this translates into a fairly direct measure of the relative distribution of normal and strange matter within the kaon; and also, importantly, its scale dependence. Further, given that the charge-conjugation operation executes $K^+ \leftrightarrow K^-$, $K^0 \leftrightarrow \bar{K}^0$, and assuming isospin symmetry (no difference between u- and d-quarks, other than their electric charge), there are just two distinct charge distributions: u in K^+ is the same as d in K^0; $\bar{s}$ in K^+ is the same as $\bar{s}$ in K^0; and these distributions also describe those in the charge-conjugated states. A third distribution is accessible in the isospin-symmetric limit, viz. the u distribution in the pion, which is the elastic pion form factor itself, and this provides an excellent counterpoint.

At low-momentum transfers, $Q^2 \lesssim 0.2$ GeV^2, charged-pion and -kaon elastic form factors, $F_M(Q^2)$, $M = \pi^+, K^+$, can be measured directly by scattering high-energy mesons from atomic electrons [5–10]. These data constrain the charge radii: $r_\pi = 0.657(12)$ fm, $r_K = 0.58(6)$ fm. The kaon is expected to be smaller because it contains the heavier s-quark [11–18]. Owing to kinematic limitations on the energy of meson beams and unfavorable momentum transfers, one must use other methods to reach higher spacelike Q^2. Meson electroproduction off nucleon targets is a reliable tool [19], which has already been used for the pion out to $Q^2 = 2.45$ GeV^2 [20–24]. Importantly, approved pion experiments [25,26] will extend this reach to $Q^2 \approx 8.5$ GeV^2, i.e. a domain upon which longstanding issues in QCD might be resolved [27]; and a forthcoming kaon experiment [28] can potentially provide kaon data out to $Q^2 \approx 5.5$ GeV^2 [29]. Existing and anticipated spacelike

*hiei@pku.edu.cn
†leichang@nankai.edu.cn
‡yxliu@pku.edu.cn
§cdroberts@anl.gov
‖tandy@kent.edu

data are complemented by measurements of e^+e^- annihilation into $\pi^+\pi^-$, K^+K^-, which afford access to pion and kaon form factors at timelike momenta out to $t \approx 17\ \mathrm{GeV}^2$ [30,31].

The impetus for measuring $F_M(Q^2)$ at large momentum transfers is a need to understand and validate a strict prediction of QCD [32–34], viz. $\exists Q_0 \gg \Lambda_{\rm QCD}$ such that

$$Q^2 F_M(Q^2) \overset{Q^2>Q_0^2}{\approx} 16\pi\alpha_s(Q^2) f_M^2 w_M^2(Q^2), \tag{1}$$

where α_s is the one-loop strong running coupling, $\Lambda_{\rm QCD} \approx 0.3$ GeV, $f_\pi = 0.092$ GeV, $f_K = 0.110$ GeV [1]; and $w_M^2 = e_{\bar q} w_{\bar q}^2(Q^2) + e_u w_u^2(Q^2)$,

$$w_f = \frac{1}{3}\int_0^1 dx \mathcal{g}_f(x)\varphi_M(x;Q^2), \tag{2}$$

$\mathcal{g}_u(x) = 1/x$, $\mathcal{g}_{\bar q}(x) = 1/(1-x)$, $e_u = 2e_{\bar q} = (2/3)$, $\bar q = \bar s$ (K^+) or $\bar d$ (π^+) and $\varphi_M(x;Q^2)$ is the meson's scale-dependent leading-twist parton distribution amplitude (PDA). The π^0 elastic form factor is identically zero owing to charge-conjugation invariance; and a prediction for the neutral kaon is obtained via $e_u \to e_d = (-1/3)$.

The value of Q_0 is not predicted by perturbative QCD; but, fortunately, continuum bound-state methods have reached the point where $F_M(Q^2)$ can be calculated directly on the entire domain of spacelike momenta, thereby enabling Q_0 to be located. This was accomplished for the pion in Ref. [27]. Herein, we both refine the method and extend it to produce a wide range of verifiable form-factor predictions, including statements, e.g. about their behavior at large timelike momenta.

II. COMPUTATIONAL METHOD

At leading order in the symmetry-preserving scheme for bound-state computations reviewed in Refs. [35,36], i.e. the Dyson-Schwinger equation rainbow-ladder (RL) truncation, kaon form factors can be computed as follows ($q = u, d$) [15]:

$$F_K(Q^2) = e_q F_K^q(Q^2) + e_{\bar s} F_K^{\bar s}(Q^2), \tag{3a}$$

$$P_\mu F_K^q(Q^2) = \mathrm{tr}_{\rm CD}\int \frac{d^4k}{(2\pi)^4}\chi_\mu^q(k+p_o,k+p_i) \times \Gamma_K(k_i;p_i)S_s(k)\Gamma_K(k_o;-p_o), \tag{3b}$$

with a similar expression for $F_K^{\bar s}(Q^2)$, where Q is the incoming photon momentum, the trace is over color and spinor indices, $p_{o,i} = P \pm Q/2$, $k_{o,i} = k + p_{o,i}/2$, $p_{o,i}^2 = -m_K^2$, m_K is the kaon mass. The calculation also requires quark propagators, S_f, $f = u(=d)$, s, which, consistent with Eq. (3b), are obtained from the rainbow-truncation gap equation; the kaon Bethe-Salpeter amplitude, Γ_K, computed in RL truncation; and consistent unamputated dressed-quark-photon vertices, χ_μ^f.

The leading-order result for $F_K(Q^2)$ is now determined once an interaction kernel is specified for the rainbow gap equation. We use that explained in Ref. [37], whose interaction strength is determined by a product: $D\omega = m_G^3$. With m_G fixed, results for properties of numerous ground-state hadrons are independent of the value of $\omega \in [0.4, 0.6]$ GeV [35–40]: we use $\omega = 0.5$ GeV. With this kernel, $f_\pi = 0.092$ GeV, $m_\pi = 0.14$ GeV and $f_K = 0.11$ GeV, $m_K = 0.49$ GeV are obtained with $m_G^{\zeta=2\ \mathrm{GeV}} = 0.87$ GeV and one-loop evolved current-quark masses $m_u^{\zeta=2\ \mathrm{GeV}} = 4.7$ MeV, $m_s^{\zeta=2\ \mathrm{GeV}} = 112$ MeV.

One may now evaluate the integrals in Eq. (3) using the algorithms introduced in Refs. [27,41]. Namely, the integrands are represented using the generalized Nakanishi interpolations of $S_{u,s}$ and Γ_K described in Ref. [42], of which the former also serve to express the unamputated photon-quark vertices, χ_μ^q [27]. With each element in Eq. (3) expressed via a generalized spectral representation, computation of $F_K(Q^2)$ reduces to the act of summing a series of terms, all of which involve a single four-momentum integral. The integrand denominator in every term is a product of k-quadratic forms, each raised to some power. Within each such term, one employs a Feynman parametrization in order to combine the denominators into a single quadratic form, raised to the appropriate power. A sensible change of variables then enables one to evaluate the four-momentum integration using standard algebraic methods. After calculation of the four-momentum integration, evaluation of the individual term is complete after one computes a finite number of simple integrals; namely, integrations over Feynman parameters and the spectral integral. The complete result for $F_K(Q^2)$ follows after summing the series.

III. RESULTS AND PROJECTIONS

The K^+ form factor, computed from Eq. (3) as described above,[1] is depicted in Figs. 1 and 2. The result is practically equivalent to that described in Ref. [15] on $Q^2 \lesssim 4\ \mathrm{GeV}^2$, which is the entire domain accessible with the algorithms employed therein. Here, however, we deliver a prediction for $F_K(Q^2)$ that extends to the entire domain of spacelike momenta; and this enables the first, realistic comparison with the prediction of Eq. (1), so long as the kaon PDA is known.

[1]For completeness, the χ_μ^f include a parameter, η_f, which modulates the dressed-quark anomalous magnetic moment [43–46]. With $\eta_u = 0.5$, $\eta_s = 0.4$, matching modern estimates [46–49]: $r_\pi = 0.66$ fm, $r_K = 0.58$ fm. Setting $\eta_u = 0 = \eta_s$ reduces $r_{\pi,K}$ by $\lesssim 3\%$ and has no visible impact on the curves drawn herein. Hence, the impact of realistic dressed-quark anomalous magnetic moments on pseudoscalar meson form factors is small [27].

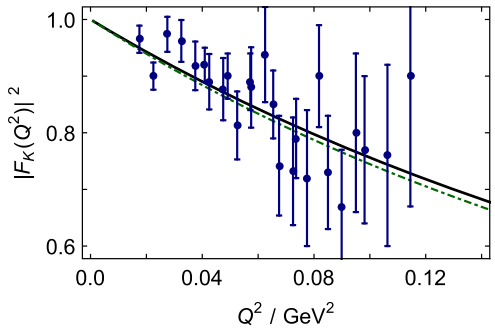

FIG. 1. Solid curve—our K^+ form factor; and dot-dashed curve (green)—result from Ref. [15]. Data: Refs. [9,10].

A simultaneous computation of π and K PDAs is reported in Ref. [42]; and pointwise forms inferred from lattice-QCD computations of the distributions' low-order Mellin moments [51,52] are reported in Refs. [29,53]. For the π, a clear picture has emerged [41,54–56]: $\varphi_\pi(x)$ is concave and markedly dilated compared to the conformal-limit result, $\varphi^{\rm cl}(x) = 6x(1-x)$, viz. in RL truncation [41],

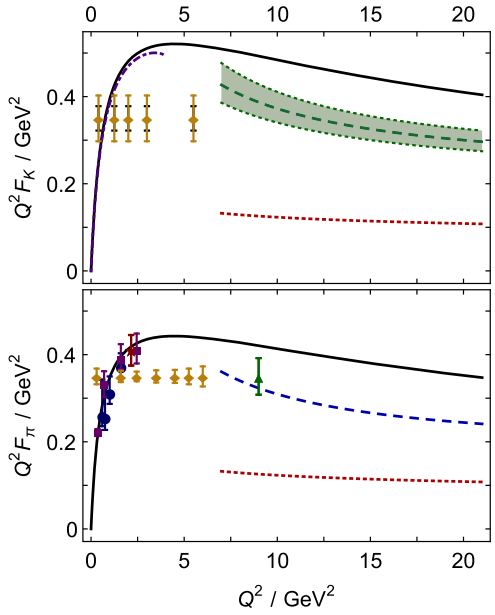

FIG. 2. Upper panel: Solid curve, Eq. (3) prediction for $Q^2F_K(Q^2)$; dot-dashed curve (indigo), result from Ref. [15], which is limited to the domain $Q^2 < 4$ GeV^2; and dashed curve and band (green), result produced by the hard scattering formula, Eqs. (1), (5). Filled diamonds, data anticipated from a forthcoming experiment [28]: The two error estimates differ in their assumptions about the t and model dependence of the form-factor extractions [29]. Lower panel: Solid curve: Prediction for $Q^2F_\pi(Q^2)$; and dashed curve (blue), result produced by the hard scattering formula, Eqs. (1), (4). Data: Star [23], circles and squares [50]; and diamonds and triangle, anticipated reach and accuracy of forthcoming experiments [25,26]. In both panels, the dotted curve (red) is Eq. (1) computed with the conformal-limit PDA, $\varphi^{\rm cl}(x) = 6x(1-x)$.

$$\varphi_\pi(x) = 1.77[x(1-x)]^{0.30}. \tag{4}$$

The K^+ PDA has similar characteristics; but, in addition, it is skewed, so that the $\bar{s}$-quark carries more of the bound-state's light-front momentum. However, the precise amount of skewing and dilation are unknown owing to disagreements between extant estimates. One may only say [29,42]: φ_K is less dilated than φ_π; and the maximum of φ_{K^+} lies in the neighbourhood of $x = 0.56$.

A benefit of our simultaneous computation of π and K form factors (Fig. 2) can be exploited here, *viz.* using Eq. (1) and the method in Ref. [19], the above constraints can be employed to determine φ_K from the computed value of $F_K(Q^2)/F_\pi(Q^2)$ on $Q^2 \simeq 8$ GeV^2, with the result

$$\varphi_K(x) = \mathcal{N}_{\alpha\beta} x^\alpha (1-x)^\beta, \qquad \alpha = 0.39(4), \qquad \beta = 0.31(4), \tag{5}$$

$\mathcal{N}_{\alpha\beta} = \Gamma(\alpha+\beta+2)/[\Gamma(\alpha+1)\Gamma(\beta+1)]$. We have introduced an error to express uncertainty in the dilation, measured by $\langle(2x-1)^2\rangle_K = 0.271(5)$. The size of the error is chosen to match that in modern lattice-QCD estimates for this moment of the pion's PDA [52]. The associated result $\langle(2x-1)\rangle_K = 0.0296(9)$ has greater uncertainty but far lesser impact [29].

Using Eq. (5) in Eq. (1) yields the (green) dashed curve and band in the upper panel of Fig. 2. Like the (blue) dashed curve in the lower panel, it is a near match in magnitude to our complete prediction, but far above the (red) dotted curve, obtained from Eq. (5) by using $w_{\bar{q}} = w_u = 1$, i.e. frozen at their conformal-limit values. Crucially, too, its evolution matches that of the RL prediction on $Q^2 \gtrsim 12$ GeV^2. Contrasting this with the evolution of the frozen-PDA conformal-limit result leads us to describe a qualitative improvement over Ref. [27].

It has long been known [33] that, while producing the right $1/Q^2$ behavior, symmetry-preserving computations via Eq. (3) (or its analogues for related processes) typically fail to generate the correct anomalous dimension and therefore yield form factors with wrong-power logarithmic scaling violations. This can be understood by noting that the meson's wave function must evolve with resolving scale just as its leading-twist PDA so that the dressed-quark and -antiquark degrees of freedom, in terms of which the wave function is expressed at a given scale Q^2, can split into less-well-dressed partons via the addition of gluons and sea quarks as prescribed by QCD dynamics. Such effects are incorporated in bound-state problems when the complete quark-antiquark scattering kernel is used; but aspects are lost when that kernel is truncated, and so it is with the RL truncation. As emphasized in recent studies of neutral pseudoscalar meson transition form factors [57,58], this is a critical flaw now that one can use QCD-connected input to make predictions at arbitrarily large Q^2 because it precludes

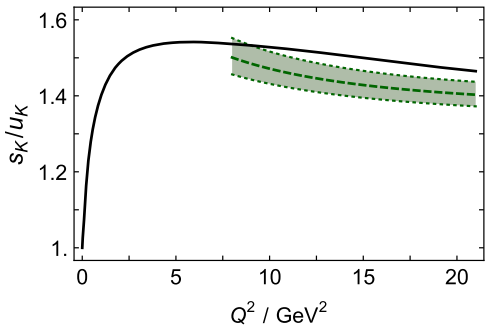

FIG. 3. Solid curve, ratio of $\bar{s}$- and u-quark contributions to the K^+ form factor; and dashed curve and band (green), prediction of the hard-scattering formula, Eqs. (1), (5).

any valid attempt to match theory with experiment. Recognizing that, Refs. [57,58] introduced a remedy; and the Appendix explains how we adapt and employ that method herein for elastic form factors.

A flavor separation of the K^+ form factor is depicted in Fig. 3. With $s_K = F_K^{\bar{s}}$, $u_K = F_K^u$ from Eq. (3a), current conservation ensures $s_K/u_K = 1$ at $Q^2 = 0$. This ratio must increase on some domain of $Q^2 > 0$ because the effective mass of a dressed s-quark is greater than that of a dressed u-quark or, equally, the lightest vector meson that can couple to a $\bar{s}\gamma_\mu s$ current (ϕ) is heavier than that which can couple to a $\bar{u}\gamma_\mu u$ current (ρ) [15,17]. Notwithstanding that, all analyses which faithfully preserve the structure of pseudoscalar meson bound-state amplitudes generated by a vector $\otimes$ vector interaction [17,59–65], thereby ensuring Eq. (3) yields internally consistent leading-twist power-law behavior, produce a ratio s_K/u_K that reaches a maximum at some nonzero value of Q^2. Thereafter, $s_K/u_K \to 1^+$. The height and location of the maximum are a measure of dynamics, and we predict a peak value $s_K/u_K \approx 1.5$ at $Q^2 \approx 6$ GeV^2. Given that Eq. (1) provides a semiquantitatively accurate description of the K^+ form factor on $Q^2 \gtrsim 8$ GeV^2 (Fig. 2), then thereupon one should also obtain a reliable estimate of s_K/u_K using the elements of the hard scattering formula. This is evidently the case.

The ratio in Fig. 3 was computed from the form factors q_K, $q = u$, s, depicted in the panels of Fig. 4, which additionally reveal some notable features of the three independent charge distributions that contribute to pion and kaon elastic electromagnetic form factors in the isospin-symmetric limit. Evidently, $u_\pi \approx u_K$ on the entire domain of spacelike Q^2. At low Q^2, this near equality was apparent in the calculation described in Ref. [15]; and our analysis reveals that it is preserved at all accessible spacelike momenta. (A similar result is obtained when using a symmetry-preserving treatment of a vector $\otimes$ vector contact interaction: see the discussion of Fig. 2 in Ref. [17].) To quantify somewhat further, one may define a charge radius via $(r_M^q)^2 = -6(dq_M/dQ^2)|_{Q^2=0}$ and obtain (in fm)

$$r_\pi^u = 0.65, \qquad r_K^u = 0.62, \qquad r_K^s = 0.43. \tag{6}$$

Plainly, $r_K^u \approx r_\pi^u$, but $r_K^s/r_K^u = 0.69 \sim M_u/M_s$, where M_q is the relevant dressed-quark mass function evaluated in the neighborhood of $k^2 = 0$. Here, then, the mass of the spectator has little impact on the charge distribution of a given light quark, and the difference between the pion and kaon form factors is almost completely determined by s_K, the charge distribution of the $\bar{s}$-quark in the K^+. The right panel of Fig. 4 also compares our predictions for q_K, $q = u$, s, with the results obtained when the hard-scattering formula is computed using the kaon PDA of Eq. (5) to calculate the factors in Eq. (2). Notably, the pattern of agreement for the flavor-separated form factors is similar to that we have already seen for the compound results;

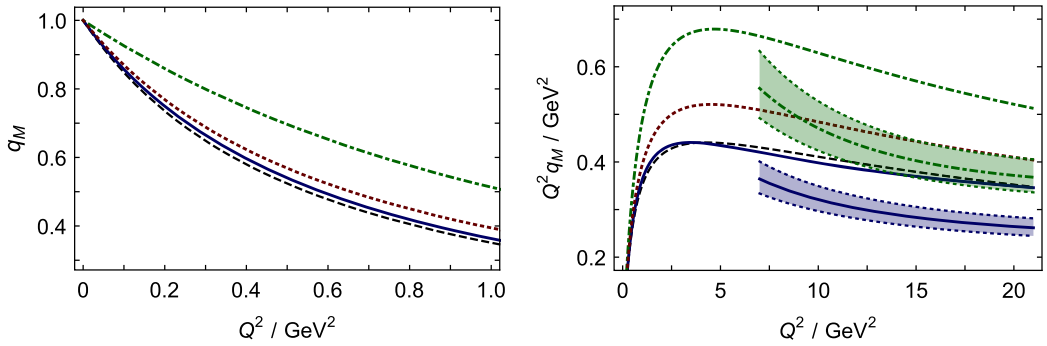

FIG. 4. Flavor separation of kaon form factor and comparison with complete π and K results. Left panel: Solid (blue) curve, $u_K = F_K^u(Q^2)$, i.e. u-quark in the K^+; dot-dashed (green) curve, $s_K = F_K^{\bar{s}}$; dashed (black) curve, $u_\pi = F_\pi$ (we assume isospin symmetry); and dotted (red) curve, F_K. Right panel: Q^2-weighted form factors. The (blue) band containing the solid (blue) curve is the hard-scattering formula prediction for $Q^2 u_K$, and the (green) band and curve correspond to $Q^2 s_K$, both obtained using Eq. (5) in Eq. (2) for the appropriate flavour and including the multiplicative factors specified in Eq. (1). Recall that quark-charge factors are not included when defining the quark contributions, Eq. (3a), so all form factors are unity at $Q^2 = 0$.

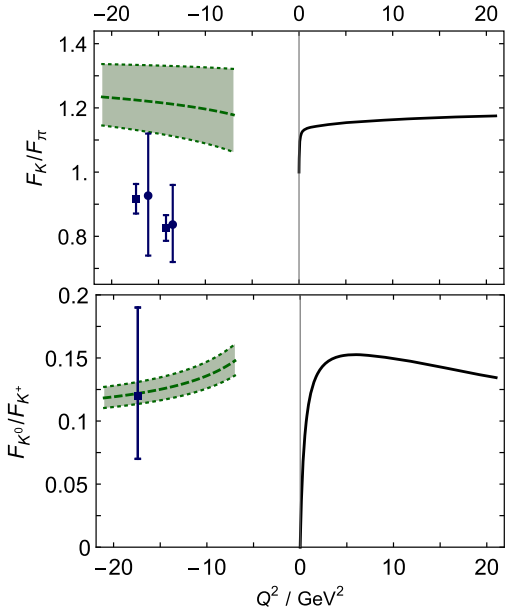

FIG. 5. Upper panel: Charged kaon-to-pion ratio. Solid curve at spacelike momenta, direct calculation, Eq. (3). Dashed curve and band (green), prediction for the timelike behavior, derived from Eqs. (1), (4), (5). Data from Ref. [30]. Lower panel: Ratio of neutral-to-charged kaon form factors. Solid curve, direct calculation. We compute $r^2_{K^0} = -(0.21\ \text{fm})^2$ *cf.* experiment [66]: $r^2_{K^0} = -(0.24 \pm 0.08\ \text{fm})^2$. Dashed curve and band (green), prediction for the timelike behavior of this ratio derived from Eqs. (1), (5). Datum from Ref. [31]: the error bar marks the 90% confidence interval.

and consequently, the QCD-scaling patterns we have highlighted are not accidental.

We depict form-factor ratios in Fig. 5. In accordance with Eq. (1), our calculated result for F_K/F_π rises logarithmically to $f_K^2/f_\pi^2 \approx 1.42$ as $Q^2 \to \infty$, whereas F_{K^0}/F_{K^+} vanishes. As was to be anticipated from Fig. 2, we predict that these conformal-limit values are inaccessible at terrestrial facilities. On the other hand, used with the PDAs appropriate to the probe scale, the hard scattering formulas are applicable. We therefore capitalize on the fact that spacelike and timelike form factors are identical at leading order in α_s, and use Eqs. (1), (4), (5) to make projections for these ratios at timelike momenta beyond the resonance region, i.e. on $t = -Q^2 \gtrsim 8\ \text{GeV}^2$. Evidently, the prediction for F_{K^0}/F_{K^+} at $t = 17.4\ \text{GeV}^2$ obtained in this way is consistent with the only existing measurement and explains it as the natural outcome of using PDAs appropriate to the scale of the experiment.

The situation is less clear for F_K/F_{π^+}: we predict $F_K/F_{\pi^+} > 1$ on $t > 8\ \text{GeV}^2$, whereas extant data lie below unity [30]. We can identify no reasonable means by which our direct computation of this ratio at spacelike momenta could be less than one at any value of Q^2: charge conservation means $F_K/F_{\pi^+} = 1$ at $Q^2 = 0$, the ordering of charge radii ensures it rises as Q^2 increases, and the absence of another set of mass scales suggests that the conformal limit ($f_K^2/f_\pi^2 \approx 1.42$) should be approached monotonically from below. These features are expressed in the semiquantitative agreement between the hard-scattering formulas and our direct calculations (Figs. 2, 3), and support the soundness of the timelike prediction based on Eqs. (1), (4), (5). Studying the separate empirical results for the π and K form factors at timelike momenta [30], one might question their normalizations because, mapped simply to spacelike momenta and compared with our direct calculations, the π measurements are a factor of ∼2 larger, and those for the K, greater by a factor of ∼1.5. Notably, a mismatch of relative normalizations would cancel in F_{K^0}/F_{K^+}. (See Ref. [67] for a complementary perspective on π and proton form factors at timelike momenta.)

IV. CONCLUDING REMARKS

Using a single bound-state interaction kernel, fully determined by just one parameter, we presented a unified description of π and K elastic form factors. This enabled us to show that, when used with PDAs computed at the probe scale, which express dynamical consequences of emergent phenomena within the SM, leading-order, leading-twist hard-scattering formulas derived for π and K elastic form factors are both accurate to 25% on $Q^2 \simeq 8\ \text{GeV}^2$, becoming more reliable as $\ln Q^2$ is increased.

Our analysis also yields projections for the separate $\bar{s}$- and u-quark contributions to the K^+ form factor. Eliminating the quark-charge weight factors, the ratio of these contributions is unity at $Q^2 = 0$, increases monotonically to a peak value of roughly 1.5 at $Q^2 \approx 6\ \text{GeV}^2$, and thereafter returns logarithmically to unity, again in agreement with the SM. We found in addition that the u-quark contributions to the π^+ and K^+ form factors are almost identical, in consequence of which the manifest difference between pion and kaon form factors is almost completely determined by the charge distribution of the $\bar{s}$-quark in the K^+.

With continuing developments in the numerical simulation of lattice-regularized quantum chromodynamics, it should be possible to validate this unified body of predictions in the foreseeable future [68,69].

Having established the domain of reliability for the hard scattering formulas, we argued that they may be used to make predictions for ratios involving π and K form factors at timelike momenta beyond the resonance region. Some data exist on this domain, but a comparison between experiment and our predictions is currently inconclusive. Notwithstanding that, the prospects for improving measurements in the timelike region are excellent given the capabilities of existing and planned e^+e^- colliders [70].

Our study reveals noticeable differences between the distribution of strange and normal matter within the strong

interaction's pseudo-Nambu-Goldstone modes. Consequently, they should serve to spur and guide new experiments at both spacelike and timelike momenta.

ACKNOWLEDGMENTS

We are grateful to R. Ent, T. Horn and C. Mezrag for insightful comments. This research was facilitated by the 2^{nd} *Sino-Americas Workshop and School on the Bound-State Problem in Continuum QCD*, Central China Normal University, Wuhan, China, and the workshop on *Novel Theory for New Facilities in Hadron Physics*, Nankai University, Tianjin, China. Research supported by the National Natural Science Foundation of China (Contracts No. 11435001 and No. 11175004); the National Key Basic Research Program of China (Contract No. G2013CB834400 and No. 2015CB856900); Government of China's Thousand Talents Plan for Young Professionals; the Chinese Ministry of Education, under the *International Distinguished Professor* programme; U.S. Department of Energy, Office of Science, Office of Nuclear Physics, under Contract No. DE-AC02-06CH11357; and National Science Foundation, under Grant No. NSF-PHY1516138.

APPENDIX: EVOLUTION OF MESON WAVE FUNCTIONS

Consider Eq. (3). If one uses $S_f(k) = 1/[i\gamma\cdot k + M_f]$, where the dressed-quark masses are constant, with $M_s \approx 1.2 M_u$, then symmetries ensure $\chi^f_\mu = S_f(k_{\rm out})\gamma_\mu S_f(k_{\rm in})$ is an adequate representation of the photon-quark vertex. The remaining element is the kaon Bethe-Salpeter amplitude. Following Refs. [18,41,59,60], one learns that realistic outcomes are ensured by

$$\Gamma_K(k;P) = \alpha_K \frac{\Lambda_K}{f_K}\left\{\int_{-1}^{1} dz \frac{\Lambda_K^2}{(k+\frac{z}{2}P)^2+\Lambda_K^2} \times \left[i\gamma_5(1+\varepsilon z)\rho_{\nu_E}(z) + g_F\gamma_5\left(\gamma\cdot P - 4\left(\frac{3}{2}+\nu_F\right)z\gamma\cdot k\right)\rho_{\nu_F}(z)\right]\right\}, \tag{A1}$$

with

$$\rho_\nu(z) = \frac{\Gamma(\frac{3}{2}+\nu)}{\sqrt{\pi}\Gamma(1+\nu)}(1-z^2)^\nu. \tag{A2}$$

The γ_5-term sets the scale of low-momentum observables; the $\gamma_5\gamma\cdot P$, $\gamma_5\gamma\cdot k$ contributions are necessary to ensure the correct form-factor power-law behavior at large momentum transfers, and they are combined with relative-weight $[-4(\frac{3}{2}+\nu_F)]$ so as to eliminate a renormalizable divergence from the integral that defines the kaon's leptonic decay constant, f_K.

With these structures in hand, one can also evaluate the kaon's leading-twist PDA:

$$f_K\varphi(x;Q^2) = {\rm tr}_{\rm CD}\int_{dk}^{Q^2} \delta_n^u(k_\eta)\gamma_5\gamma\cdot n\chi_K(k_\eta,k_{\bar\eta}), \tag{A3}$$

where $\int_{dk}^{Q^2}$ is a Poincaré-invariant regularization of the four-dimensional integral, with Q^2 setting the PDA's scale; $\delta_n^u(k_\eta) = \delta(n\cdot k_\eta - x n\cdot P)$, $n^2=0$, $n\cdot P = -m_K$;

$$\chi_K(k_\eta,k_{\bar\eta}) = S_u(k_\eta)\Gamma_P(k_{\eta\bar\eta};P)S_s(k_{\bar\eta}), \tag{A4}$$

$k_{\eta\bar\eta} = [k_\eta + k_{\bar\eta}]/2$, $k_\eta = k+\eta P$, $k_{\bar\eta} = k-(1-\eta)P$, $\eta\in[0,1]$. Inserting Eq. (A1) in Eq. (A3), one arrives at an algebraic result:

$$\varphi(x;Q^2) = \mathcal{n}_{\alpha\beta}x^\alpha(1-x)^\beta, \tag{A5}$$

where the Q^2-dependent exponents α, β are fixed by the values of ν_E and ε in Eq. (A1).

Now, setting $m_K = 0.49$ GeV and $Q^2 = 4\ {\rm GeV}^2 =: Q_2^2$, one obtains unit charge, $f_K = 0.11$ GeV, and the PDA in Eq. (5) with $M_u = 0.4$ GeV, $\Lambda_K = 1.1 M_u$, $\nu_E = -0.78$, $\nu_F = 1$, $g_F = 0.1\ {\rm GeV}^{-1}$, $\varepsilon = 0.10$, $\alpha_K = 1.48$.

It is now straightforward to chart the impact on the kaon form factor of leading-order QCD evolution [32–34]. One evolves the PDA from Q_2^2 to some new value, Q^2. The evolved PDA may still be expressed using Eq. (A5) and can therefore be recovered using Eqs. (A1), (A3) so long as evolved values of ν_E and ε are used. In fact, on the domain $Q_2^2 < Q^2 \le 40\ {\rm GeV}^2$ one may use $\varepsilon =$ constant; and the impact of evolution is accurately incorporated simply by using ($\zeta^2 = Q^2 - Q_2^2$):

$$\nu_E(\zeta^2) = -\frac{0.78 + 0.059\zeta^2}{1+0.098\zeta^2}. \tag{A6}$$

Thus informed, one evaluates the $\bar s$- and u-quark contributions to the K^+ form factor, defined by Eq. (3), on $\zeta^2 > 0$, using the simple propagators and vertices described above and $\nu_E(\zeta^2)$ from Eq. (A6) in the expression for the Bethe-Salpeter amplitude, Eq. (A1). Normalizing to the values at $\zeta^2 = 0$, one obtains the following evolution functions for these separate contributions:

$$\mathcal{E}_{u_K}(\zeta^2>0) = \frac{1+0.10\zeta^2+0.0011\zeta^4}{1+0.12\zeta^2+0.0019\zeta^4}, \tag{A7a}$$

$$\mathcal{E}_{s_K}(\zeta^2>0) = \frac{1+0.033\zeta^2-0.000011\zeta^4}{1+0.049\zeta^2+0.000044\zeta^4}. \tag{A7b}$$

Our final results for the meson form factors are obtained by incorporating these evolution factors into the individual pieces of Eq. (3a):

$$F_K^f(Q^2) = \hat{F}_K^f(Q^2) \times [\theta(Q_2^2 - Q^2) + \theta(Q^2 - Q_2^2)\mathcal{E}_{f_K}(Q^2 - Q_2^2)], \tag{A8}$$

where $\hat{F}_K^f(Q^2)$ is the result obtained directly from Eq. (3b). At $Q^2 = 20\ \mathrm{GeV}^2$, each of these functions introduces a ∼15% suppression.

The procedure described in this appendix [57,58] assumes that the dressed-quark degrees of freedom defined by a RL computation renormalized at $Q_2^2 = 4\ \mathrm{GeV}^2$ capture all relevant dynamics below that scale, an assumption supported by comparisons with extant data, and thereafter enables those degrees of freedom to evolve as prescribed by QCD. As Figs. 2, 3 demonstrate, the method repairs a known failing [33] of symmetry-preserving computations of meson form factors via Eq. (3), *viz.* it solves the problem of wrong-power logarithmic scaling violations. The method is readily simplified to suit the pion.

[1] C. Patrignani *et al.*, Chin. Phys. C **40**, 100001 (2016).
[2] M. S. Bhagwat, M. A. Pichowsky, C. D. Roberts, and P. C. Tandy, Phys. Rev. C **68**, 015203 (2003).
[3] P. O. Bowman, U. M. Heller, D. B. Leinweber, M. B. Parappilly, A. G. Williams, and J. Zhang, Phys. Rev. D **71**, 054507 (2005).
[4] M. S. Bhagwat and P. C. Tandy, AIP Conf. Proc. **842**, 225 (2006).
[5] E. B. Dally *et al.*, Phys. Rev. D **24**, 1718 (1981).
[6] E. B. Dally *et al.*, Phys. Rev. Lett. **48**, 375 (1982).
[7] S. R. Amendolia *et al.*, Nucl. Phys. **B277**, 168 (1986).
[8] S. R. Amendolia *et al.*, Phys. Lett. **146B**, 116 (1984).
[9] E. Dally *et al.*, Phys. Rev. Lett. **45**, 232 (1980).
[10] S. Amendolia *et al.*, Phys. Lett. B **178**, 435 (1986).
[11] R. Tarrach, Z. Phys. C **2**, 221 (1979).
[12] C. R. Ji and S. R. Cotanch, Phys. Rev. D **41**, 2319 (1990).
[13] F. Cardarelli, I. L. Grach, I. M. Narodetskii, E. Pace, G. Salmè, and S. Simula, Phys. Lett. B **332**, 1 (1994).
[14] C. J. Burden, C. D. Roberts, and M. J. Thomson, Phys. Lett. B **371**, 163 (1996).
[15] P. Maris and P. C. Tandy, Phys. Rev. C **62**, 055204 (2000).
[16] E. O. da Silva, J. P. B. C. de Melo, B. El-Bennich, and V. S. Filho, Phys. Rev. C **86**, 038202 (2012).
[17] C. Chen, L. Chang, C. D. Roberts, S. M. Schmidt, S. Wan, and D. J. Wilson, Phys. Rev. C **87**, 045207 (2013).
[18] C. Chen, L. Chang, C. D. Roberts, S. Wan, and H.-S. Zong, Phys. Rev. D **93**, 074021 (2016).
[19] S.-X. Qin, C. Chen, C. Mezrag, and C. D. Roberts, arXiv: 1702.06100.
[20] J. Volmer *et al.*, Phys. Rev. Lett. **86**, 1713 (2001).
[21] T. Horn *et al.*, Phys. Rev. Lett. **97**, 192001 (2006).
[22] V. Tadevosyan *et al.*, Phys. Rev. C **75**, 055205 (2007).
[23] T. Horn *et al.*, Phys. Rev. C **78**, 058201 (2008).
[24] H. P. Blok *et al.*, Phys. Rev. C **78**, 045202 (2008).
[25] G. M. Huber and D. Gaskell, Jefferson Lab Experiment Proposal No. E12-06-101, 2006.
[26] T. Horn and G. M. Huber, Jefferson Lab Experiment Proposal No. E12-07-105, 2007.
[27] L. Chang, I. C. Cloët, C. D. Roberts, S. M. Schmidt, and P. C. Tandy, Phys. Rev. Lett. **111**, 141802 (2013).
[28] T. Horn *et al.*, Approved Jefferson Lab 12 GeV Experiment, 2009 (unpublished).
[29] T. Horn and C. D. Roberts, J. Phys. G **43**, 073001 (2016).
[30] K. K. Seth, S. Dobbs, Z. Metreveli, A. Tomaradze, T. Xiao, and G. Bonvicini, Phys. Rev. Lett. **110**, 022002 (2013).
[31] K. K. Seth, S. Dobbs, A. Tomaradze, T. Xiao, and G. Bonvicini, Phys. Lett. B **730**, 332 (2014).
[32] G. P. Lepage and S. J. Brodsky, Phys. Lett. **87B**, 359 (1979).
[33] G. P. Lepage and S. J. Brodsky, Phys. Rev. D **22**, 2157 (1980).
[34] A. V. Efremov and A. V. Radyushkin, Phys. Lett. **94B**, 245 (1980).
[35] P. Maris and C. D. Roberts, Int. J. Mod. Phys. E **12**, 297 (2003).
[36] L. Chang, C. D. Roberts, and P. C. Tandy, Chin. J. Phys. (Taipei) **49**, 955 (2011).
[37] S.-X. Qin, L. Chang, Y.-X. Liu, C. D. Roberts, and D. J. Wilson, Phys. Rev. C **84**, 042202(R) (2011).
[38] G. Eichmann, R. Alkofer, I. C. Cloët, A. Krassnigg, and C. D. Roberts, Phys. Rev. C **77**, 042202(R) (2008).
[39] G. Eichmann, I. C. Cloët, R. Alkofer, A. Krassnigg, and C. D. Roberts, Phys. Rev. C **79**, 012202(R) (2009).
[40] S.-X. Qin, L. Chang, Y.-X. Liu, C. D. Roberts, and D. J. Wilson, Phys. Rev. C **85**, 035202 (2012).
[41] L. Chang, I. C. Cloët, J. J. Cobos-Martinez, C. D. Roberts, S. M. Schmidt, and P. C. Tandy, Phys. Rev. Lett. **110**, 132001 (2013).
[42] C. Shi, C. Chen, L. Chang, C. D. Roberts, S. M. Schmidt, and H.-S. Zong, Phys. Rev. D **92**, 014035 (2015).
[43] J. Singh, Phys. Rev. D **31**, 1097 (1985).
[44] N. I. Kochelev, Phys. Lett. B **426**, 149 (1998).
[45] P. J. A. Bicudo, J. E. F. T. Ribeiro, and R. Fernandes, Phys. Rev. C **59**, 1107 (1999).
[46] L. Chang, Y.-X. Liu, and C. D. Roberts, Phys. Rev. Lett. **106**, 072001 (2011).
[47] A. Bashir, R. Bermúdez, L. Chang, and C. D. Roberts, Phys. Rev. C **85**, 045205 (2012).
[48] S.-X. Qin, L. Chang, Y.-X. Liu, C. D. Roberts, and S. M. Schmidt, Phys. Lett. B **722**, 384 (2013).
[49] L. Chang, I. C. Cloët, C. D. Roberts, and H. L. L. Roberts, AIP Conf. Proc. **1354**, 110 (2011).
[50] G. Huber *et al.*, Phys. Rev. C **78**, 045203 (2008).

[51] R. Arthur, P. A. Boyle, D. Brömmel, M. A. Donnellan, J. M. Flynn, A. Jüttner, T. D. Rae, and C. T. C. Sachrajda, Phys. Rev. D **83**, 074505 (2011).
[52] V. M. Braun, S. Collins, M. Göckeler, P. Pérez-Rubio, A. Schäfer, R. W. Schiel, and A. Sternbeck, Phys. Rev. D **92**, 014504 (2015).
[53] J. Segovia, L. Chang, I. C. Cloët, C. D. Roberts, S. M. Schmidt, and H.-s. Zong, Phys. Lett. B **731**, 13 (2014).
[54] S. Mikhailov and A. Radyushkin, JETP Lett. **43**, 712 (1986).
[55] S. J. Brodsky and G. F. de Teramond, Phys. Rev. Lett. **96**, 201601 (2006).
[56] J.-H. Zhang, J.-W. Chen, X. Ji, L. Jin, and H.-W. Lin, Phys. Rev. D **95**, 094514 (2017).
[57] K. Raya, L. Chang, A. Bashir, J. J. Cobos-Martinez, L. X. Gutiérrez-Guerrero, C. D. Roberts, and P. C. Tandy, Phys. Rev. D **93**, 074017 (2016).
[58] K. Raya, M. Ding, A. Bashir, L. Chang, and C. D. Roberts, Phys. Rev. D **95**, 074014 (2017).
[59] P. Maris and C. D. Roberts, Phys. Rev. C **56**, 3369 (1997).
[60] P. Maris and C. D. Roberts, Phys. Rev. C **58**, 3659 (1998).
[61] L. X. Gutiérrez-Guerrero, A. Bashir, I. C. Cloët, and C. D. Roberts, Phys. Rev. C **81**, 065202 (2010).
[62] H. L. L. Roberts, C. D. Roberts, A. Bashir, L. X. Gutiérrez-Guerrero, and P. C. Tandy, Phys. Rev. C **82**, 065202 (2010).
[63] H. L. L. Roberts, A. Bashir, L. X. Gutiérrez-Guerrero, C. D. Roberts, and D. J. Wilson, Phys. Rev. C **83**, 065206 (2011).
[64] F. E. Serna, M. A. Brito, and G. Krein, AIP Conf. Proc. **1701**, 100018 (2016).
[65] M. A. Bedolla, K. Raya, J. J. Cobos-Martínez, and A. Bashir, Phys. Rev. D **93**, 094025 (2016).
[66] W. R. Molzon, J. Hoffnagle, J. Roehrig, V. L. Telegdi, B. Winstein, S. H. Aronson, G. J. Bock, D. Hedin, G. B. Thomson, and A. Gsponer, Phys. Rev. Lett. **41**, 1213 (1978).
[67] A. P. Bakulev, A. V. Radyushkin, and N. G. Stefanis, Phys. Rev. D **62**, 113001 (2000).
[68] J. Koponen, A. C. Zimermmane-Santos, C. T. H. Davies, G. P. Lepage, and A. T. Lytle, arXiv:1701.04250.
[69] A. J. Chambers *et al.*, arXiv:1702.01513.
[70] R. Holt and R. Gilman, Rep. Prog. Phys. **75**, 086301 (2012).